FR9800244

I.P.N. - 91406 ORSAY CEDEX

institut de physique nucléaire CNRS - IN2P3 UNIVERSITÉ PARIS - SUD

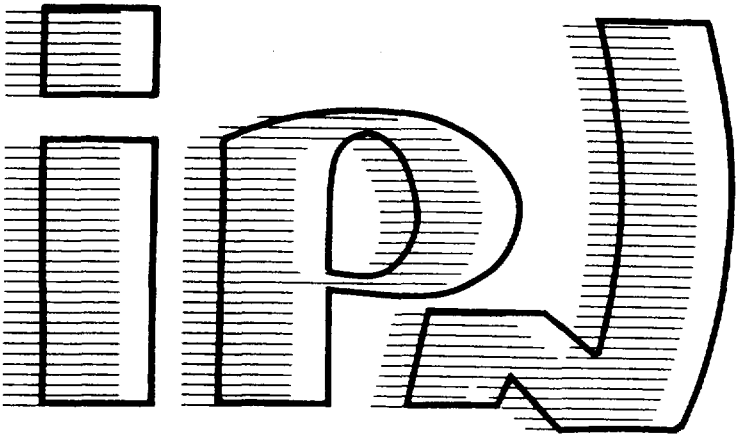

IPNO 97-04

SIMULATION OF NEUTRON RICH NUCLEI PRODUCTION THROUGH ^{239}U FISSION AT INTERMEDIATE ENERGIES

M. Mirea, F. Clapier, N. Pauwels and J. Proust

Simulation of Neutron Rich Nuclei Production through ^{239}U Fission at Intermediates Energies

M. Mirea*, F. Clapier, N. Pauwels, J. Proust
Institut de Physique Nucléaire – Orsay

November 27, 1997

Abstract

We describe the theoretical part and some results obtained from a model realised for fission processes in wide range of mass–asymmetries. The fission barriers are computed in a tridimensional configuration space using the Yukawa – plus – exponential macroscopic energies corrected within the Strutinsky procedure. It is assumed that channel probabilities are proportional with Gamow penetrabilities. The model is applied for the disintegration of the ^{239}U in order to determine the relative yields for the production of neutron rich nuclei at diverse intermediate energies.

I. INTRODUCTION

A few years ago, an ongoing program was started in order to produce neutron rich beams obtained through fission processes induced by fast neutrons [1]. These neutrons are obtained by breaking up an intense deuteron beam in a dedicated converter. The aim of this program is the investigation of the optimum conditions for the production of neutron–rich fission fragment beams extracted from thick targets. The challenge consists in the R&D for a device in which the produced activities are transferred to an ion–source with high efficiency. This will be crucial for the viability of projects like the one proposed by the National Argonne Laboratory [2]. It will also be of high interest for radioactive beam facilities under construction [3, 4], like SPIRAL at GANIL, which may benefit from an intense deuteron beam.

An appropriate theoretical tool for estimations of fission products towards neutron drip line is needed in order to investigate the optimum conditions of their production in connexion with the excitation energy and the reaction channel. In the following, such a model developed in the frame of PARRNE [1] (Production d'Atomes Radioactifs Riches en Neutrons) projet is described. For the time being, the variation of the neutron rich nuclei relative yields are studied as a function of the excitation energy of the parent nucleus ^{239}U to try the determination of optimum production conditions. These nuclei are produced in our experiments by bombarding the ^{238}U with the intense secondary neutron flux obtained by breaking up a deuteron beam in a Be converter. For the simulation purposes, the range of the excitation energy was choosed in the interval [5–100] MeV.

*Permanent adress: Institut de Physique et Ingénierie Nucléaire – Bucarest, Roumanie

II. FORMALISM

We realised a code able to calculate the relative probabilities for the formation of a binary system of two different nuclei characterized by different mass and charges (A_1, Z_1) and (A_2, Z_2) from a parent nucleus (A_0, Z_0) as function of its excitation energy.

II.1. Nuclear shape parametrization

The nuclear parametrization is defined by joining smoothly two intersecting spheres of radius R_1 and R_2 with a neck surface generated by the rotation of a circle of radius R_3 around the symmetry axis, as presented in figure 1. The distance between the center of this circle and the axis of symmetry is given by ρ_3. By imposing the condition of volume conservation, the surface is perfectly determined by the values of the parameters R (distance between the centers of the spheres), R_3 (the radius of the neck) or $C = S/R_3$ (where $S = +1$ when $\rho_3 - R_3 \geq 0$ and $S = -1$ when $\rho_3 - R_3 < 0$) and R_2 (the radius of the emitted fragment). These three parameters characterize the elongation, the necking and the mass-asymmetry, respectively. Due to the axial-symmetry of this system, the surface equation is given in cylindrical coordinates:

$$\rho_s(z) = \begin{cases} [R_1^2 - (z - z_1)^2]^{1/2} & z \leq z_{c1} \\ \rho_3 - S\,[R_3^2 - (z - z_3)^2]^{1/2} & z_{c1} < z < z_{c2} \\ [R_2^2 - (z - z_2)^2]^{1/2} & z \geq z_{c2} \end{cases} \quad (1)$$

For extremely large values of R_3, that means for $C = S/R_3 \approx 0$ fm^{-1} the parametrization in the interval $z_{c1} < z < z_{c2}$ is described by relation:

$$\rho_s(z) = [a(z - z_{c1}) + b]^{1/2}$$

with

$$a = \{[R_2^2 - (z_{c2} - z_2)^2]^{\frac{1}{2}} - [R_1^2 - (z_{c1} - z_1)^2]^{\frac{1}{2}}\}/(z_{c2} - z_{c1})$$

$$b = [R_1^2 - (z_{c1} - z_1)^2]^{\frac{1}{2}}$$

The significance of all the geometrical symbols are presented by means of figure 1. The subscripts 0, 1 and 2 help to assign the parent, daughter and the emitted nuclei, respectively. The initial radius of the parent is $R_0 = r_0 A_0^{1/3}$, the final radii of the two fragments are $R_{if} = r_0 A_i^{1/3}$, with $i = 1, 2$ and the constant radius $r_0 = 1.16$ fm. In equation (1), ρ_s denotes the value of the coordinate ρ on the nuclear surface. "Diamond"- like shapes are obtained for $S = -1$ and necked-in shapes for $S = +1$. When $S = -1$, the volume of the emitted fragment V_2 is always computed in the interval $[z_{c2}, z_2 + R_2]$. In the case $S = +1$ we compute this volume between $[z_{c2}, z_2 + R_2]$ when $z_{c2} \leq z_3$ and between $[z_3, z_2 + R_2]$ when $z_{c2} \geq z_3$. During the deformation process, the condition of volume conservation $V_1 + V_2 = V_0$ is preserved. When $R_3 = 0.$ fm, the simple parametization of two intersecting spheres is obtained. This nucleus shape parametrization was widely used in nuclear dynamic calculations [5] in a large range of mass asymmetries because it accounts for the most important degrees of freedom encountered in fission processes: elongation, necking and mass–asymmetry. In the following, sometimes, in place of R we use $R_n = (R - R_i)/(R_f - R_i)$ which defines the normalised coordinate of elongation. Here $R_i = R_0 - R_{2f}$ represents

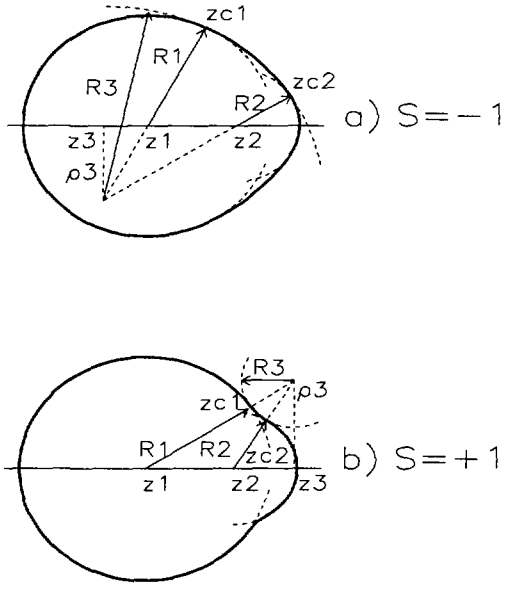

Figure 1: Nuclear shape parametrization

always the initial moment when a nascent fragment starts to escape from the spherical parent nucleus and $R_f = R_{1f} + R_{2f}$ represents the touching point configuration when the two fragments have a spherical shape.

A single trajectory in the configuration space is used for all the channels, i.e., the dependence of R_3 as function of R is the same for all the processes. This trajectory assumes that, during the fission process, the nucleus has a prolate deformation with a very large neck radius R_3 The scission is approximatively achieved when the neck radius reaches zero. The sequence of nuclear shapes during the fission process for the disintegration of a parent nucleus with mass A_0=239 in two fragments with masses 96 and 143 is shown in figure 2. In this representation the normalised elongation coordinate R_n begins at 0 and varies with 0.1 steps.

II.2. Macroscopic deformation energy

The deformation energy was computed in the framework of the Yukawa–plus–exponential [6] model extended for binary systems with different charge densities [7] where another degree of freedom is introduced, namely the charge asymmetry. The charge density of the system is kept initially unchanged, and in the final stages of the process where very necked forms are reached, the charge densities of the two fragments are linearly varying function of R up to their final values in the output channel. This behaviour is suggested by the experimental observation of a fast equilibration processes. The potential has been used in 1979 in one of the three variants of the numerical superasymmetric fission model developed to study α-decay as a fission process. We are now employing updated values of the numerical parameters [8]. Both nuclear, E_n,

$$E_n = -\frac{a_2}{8\pi^2 r_0^2 a^4}\int_V\int_V\left(\frac{r_{12}}{a}-2\right)\frac{\exp\left(-\frac{r_{12}}{a}\right)}{\frac{r_{12}}{a}}d^3r_1 d^3r_2 \qquad (2)$$

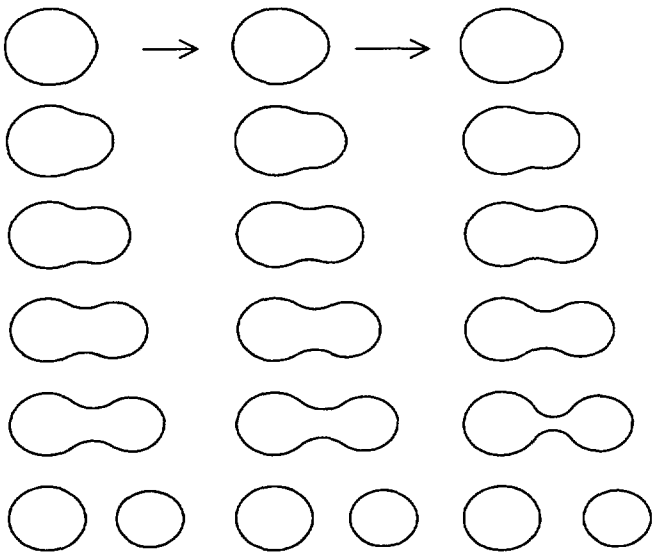

Figure 2: Sequence of nuclear shapes during the process.

and Coulomb, E_c,

$$E_c = \frac{1}{2}\int_\infty \int_\infty \frac{\rho_e(\vec{r_1})\rho_e(\vec{r_2})}{r_{12}} d^3r_1 d^3r_2 \tag{3}$$

(with $r_{12} = \mid \vec{r_1} - \vec{r_2} \mid$) energies are expressed as a sum of three shape dependent terms: the self–energies of the fragments (B_{ni}, B_{ci}, i=1,2), plus the interaction energy (B_{n12}, B_{c12}):

$$E_n/E_n^0 = (c_{s1}/c_s)B_{n1} + [(c_{s1}c_{s2})^{1/2}/c_s]B_{n12} + (c_{s2}/c_s)B_{n2} \tag{4}$$

$$E_c/E_c^0 = (\rho_{1e}/\rho_{0e})^2 B_{c1} + (\rho_{1e}\rho_{2e}/\rho_{0e}^2)B_{c12} + (\rho_{2e}/\rho_{0e})^2 B_{c2} \tag{5}$$

where E_n^0 and E_c^0 correspond to the spherical shapes, ρ_{ie} are charge densities and

$$c_{si} = a_s[1 - \kappa_s(N_i - Z_i)^2/A_i^2] \tag{6}$$

$$\rho_{ie} = 3eZ_i/(4\pi r_0^3 A_i) \tag{7}$$

with the parameters: $a_s = 21.13$ MeV, $\kappa_s = 2.3$, $a = 0.68$ fm, $a_V = 15.9937$ MeV, $\kappa_V = 1.927$. The quantities B_{ni} and B_{ci} in the above equations are dependent on nuclear shape; their expressions containing two- and threefold integrals are evaluated by numerical quadrature.

Further more, the contribution of the volume energy is added

$$E_V = E_{V1} + E_{V2} - E_{V0} \tag{8}$$

where

$$E_{Vi} = -a_V[1 - \kappa_V(N_i - Z_i)^2/A_i^2] \tag{9}$$

The interaction energy of two spherical nuclei may be found by using analytical relationships. So, the total deformation macroscopic energy becomes:

$$E_{\rm LDM} = E_n + E_c + E_V - E_0 \tag{10}$$

The microscopic energy must be added to this macroscopic potential.

II.3. Level scheme

The energetic levels are obtained with an improved version of the superasymmetric two–center shell model (STCM) [9, 10].

For the nuclear shape parametrisation presented above, the microscopic potential (in cylindrical coordinates) is split into several parts which are treated separately:

$$V(\rho,z,\varphi) = V_0(\rho,z) + V_{as}(\rho,z) + V_n(\rho,z) + V_{Ls}(\rho,z,\varphi) + V_{L^2}(\rho,z,\varphi) - V_c \tag{11}$$

where $V_0(\rho,z)$ represents the two–center harmonic potential whose eigenvectors can be analytically obtained by solving the Schrödinger's equation. It is given by the relation:

$$V_0(\rho,z) = \begin{cases} \frac{1}{2}m_0\omega_{z1}^2(z+z_1)^2 + \frac{1}{2}m_0\omega_\rho^2\rho^2, & z<0 \\ \frac{1}{2}m_0\omega_{z2}^2(z-z_2)^2 + \frac{1}{2}m_0\omega_\rho^2\rho^2, & z\geq 0 \end{cases} \tag{12}$$

where m_0 is the nucleon mass, z_1, z_2 (reals, positives) represent the distances between the centers of the spheroïds and their intersection plane and ω_i is the oscillator stiffness.

The role played by the other terms in the total potential, i.e., V_{as}, V_n, V_{ls}, V_{l^2}, V_c is related to the mass-asymmetry, to the necking, to the spin orbit coupling, to the l^2 correction and to the depth of the potential, respectively and are defined as in Ref. [9]. The mass–asymmetry term is the same as that used in Ref. [10].

Due to the cylindric symmetry of the system, the quantum numbers along the ρ–axis (n_ρ) and φ–coordinates (m) are constants of the motion.

The spin orbit and l^2 coefficients are obtained from Ref. [12] by interpolating the published values as funtion of their mass.

II.4. Shell effects

The shell effects are computed using the well known Strutinsky procedure [11]. The total energy is the sum of the liquid drop energy and the shell and pairing effects due to the protonic and neutronic level schemes.

The shell correction is:

$$\delta V_{\mathrm{p(n)}} = [2\sum_\nu \epsilon_\nu - 2\int_{-\infty}^{\tilde{\lambda}} \epsilon\tilde{g}\, d\epsilon] \tag{13}$$

where ϵ_ν are the single–particle energies, $\tilde{\lambda}$ is the smoothed Fermi energy,

$$\tilde{g} = \frac{1}{\tilde{\gamma}}\int_{-\infty}^{\infty} \mathcal{F}(\frac{\epsilon-\epsilon'}{\tilde{\gamma}})\sum_\nu \delta(\epsilon-\epsilon_\nu)d\epsilon' \tag{14}$$

is the mean density of single particle levels, $\tilde{\gamma}$ is an interval around the Fermi energy which is taken 1.15 (in $\hbar\omega$ units) times the value of the mean distance between the major shells of the light fragment, while

$$\mathcal{F}(x) = \frac{1}{\pi^{1/2}}\exp(-x^2)\sum_{k=0,2}^{2m} a_k H_k(x^2)$$

is the well known Strutinsky smoothing function with Hermite polynomials. The sum over ν means for all the levels with energies below the Fermi value. The smooth value of the Fermi energy $\tilde{\lambda}$ is obtained as usual from the condition of number conservation. For odd nuclei the procedure becomes a little more complicated. We perform the estimation for the even neighbouring system and we compute the difference given by relation (13) only for the odd nucleon. This latter value is added to the shell correction.

The pairing correction is for [protons – indice p and for neutrons – indice n]:

$$\delta P_{\mathrm{p(n)}} = P - \frac{1}{2} g(\tilde{\lambda})\tilde{\Delta}^2 \tag{15}$$

where P is the value obtained directely from the level sheme while the smoothed distribution gap parameter $\tilde{\Delta}$ is deduced from the BCS equation on the form:

$$\frac{2}{G} = \int_{\tilde{\lambda}-\Omega}^{\tilde{\lambda}+\Omega} \frac{\tilde{g}d\epsilon}{[(\epsilon-\tilde{\lambda})^2+\tilde{\Delta}^2]^{1/2}} = 2\tilde{g}\ln(\frac{2\Omega}{\tilde{\Delta}}) \tag{16}$$

and Ω is an energetic interval of the order of $\tilde{\gamma}$ and G represents the pairing strenght.

For odd filled level we appealed to the blocking effect in computing this correction.

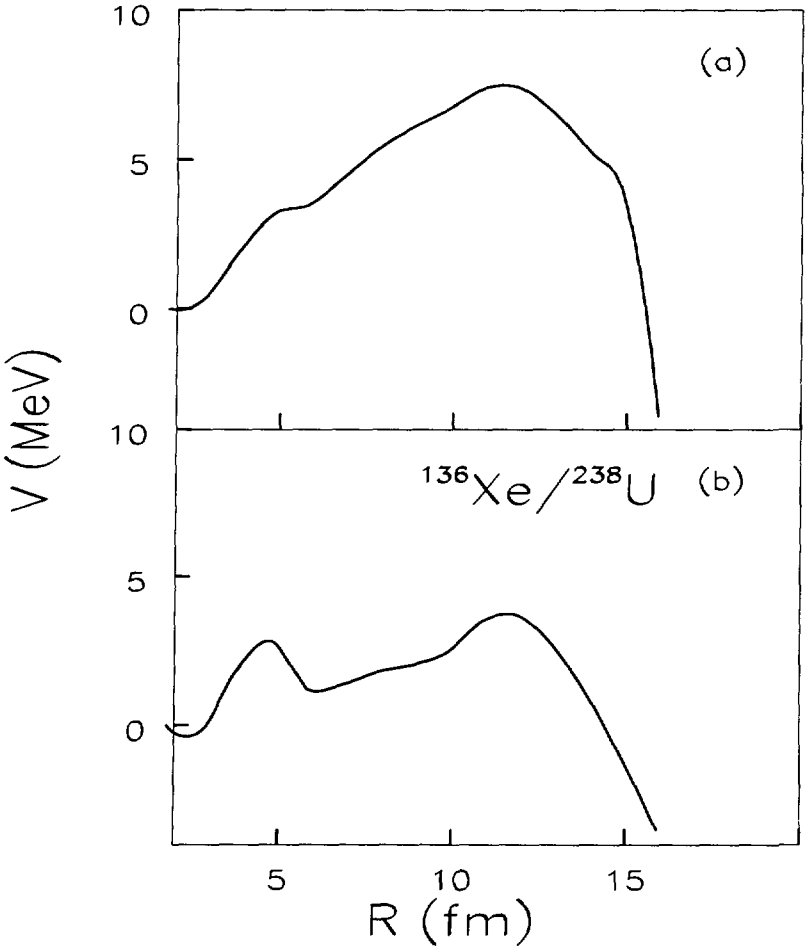

Figure 3: Potential energy in the ground state (b) and in the excited state (a) at an excitation energy of 100 MeV during the disintegration of the ^{238}U with heavy fragment ^{136}Xe.

We use the Franck–Condon principle in a sense similar to that presented in Ref. [14] where it is evidenced that in an ideal colective model, the excitation process takes place in such a way that the positions and velocities coordinates of the heavy part of the system remains unchanged. At a fixed value of the deformation coordinates we assume the system shifts from one potential to another.

The excitation energy will damp the shell effects. For simplicity, we assume an exponential decay [13]

$$U_{\rm tot} = E_{\rm LDM} + \delta U(T=0)\exp(-T^2/T_0^2) \tag{17}$$

where $E_{\rm LDM}$ is the liquid drop potential along the trajectory path and $\delta U = \delta V_p + \delta V_n + \delta P_p + \delta P_n$ is the sum of shell and pairing corrections (for both neutronic and protonic scheme) calculated for the ground state. The nuclear temperature T is connected with the excitation energy

$$E^* = A_0 T^2/(10\ {\rm MeV}) \tag{18}$$

where the value T_0=1.5 MeV allows the shell corrections vanish if $E^* > 60$ MeV. A comparison between the nuclear shape of the barrier in the ground state and at an excitation energy of 100 MeV is displayed in figure 3. So, when the nucleus is excited, according to the Franck–Condon effect, the system will skip from ground state potential energy to another one characterized by its nuclear temperature.

II.5. Penetrabilities

The multidimensional fission penetrability P is calculated in the semi-classical Wentzel–Kramers–Brillouin (WKB) method. The region of interest is classical forbidden. The integral is computed for a given energy which connects one point in the ground state and the exit point from the barrier, called end or turning points, along a classical trajectory in the configuration space.

The action integral during the disintegration can be written:

$$K_{ov} = \frac{2}{\hbar}\int_{R_a}^{R_b}\sqrt{2BE(R,C,R_2)}dR \tag{19}$$

where R_a and R_b are the turning points, B is the reduced mass of the system $B = A_1A_2/A_0$ and $E = U_{\rm tot} - E_{\rm g.s.} - E_v - E_{\rm mac}$ is the high of the forbidden barrier. $U_{\rm tot}$ is defined by Rel. (17), $E_{\rm g.s.}$ is the lower state of the whole system at a given temperature (it corresponds to the ground state energy at T=0), E_v = 0.5 MeV is the zero point vibration energy and $E_{\rm mac}$ = 1.5 MeV is the macroscopic kinetic energy.

The purpose of calculations dealing with minimal action principle is to obtain the lower value of this integral by finding a least action trajectory between the end points determined by the given value of the energy and also for any variation of the initial conditions in the turning points. It is considered that the path for the minimal action is the same for all the channels as discussed in section II.1. Our goal is to deduce for a given excitation energy the two or four (if the second minima of the barrier is below the energy of the first turning point) turning points which determine the value of the action integral and after that to compute the penetrabilities of a given channel. Afterwards, for a given excitation energy it is assumed that the the yield of a given nuclide formation is proportional to the penetrability. In this way, relative yields can be obtained.

III. RESULTS AND DISCUSSION

The channel preformation fulfills two requirements. First of all, the blocking effect is computed taking into account the fact that unpaired nucleons of the two nascent fragments preserve their spin projection Ω during the decay and after the separation. In other words, the excitation of the parent nucleus ^{239}U from its ground state is realised in such a manner that the unpaired nucleons have the same values of its spin projection Ω and of the quantum numbers n_ρ and m as those in the ground state of the final fragments. Secondly, the light fragment maintains its radius during all the process.

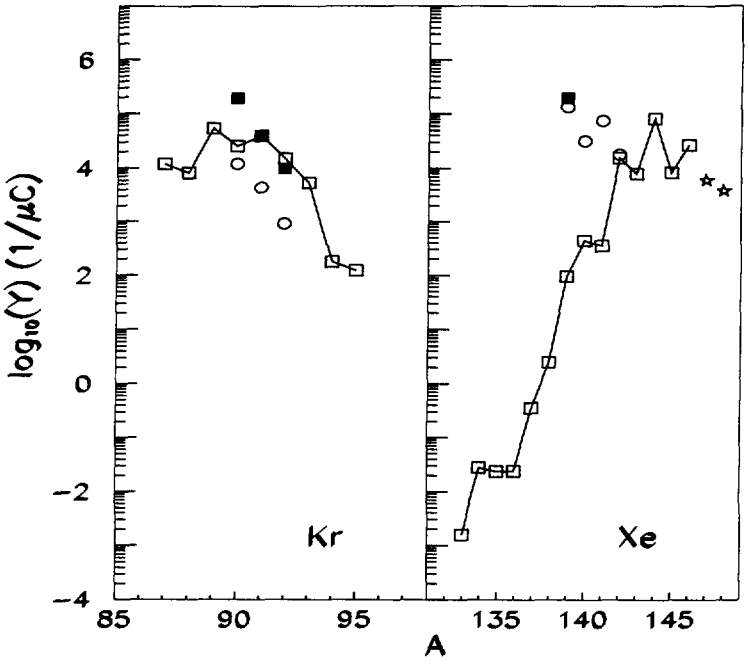

Figure 4: Filled squares: the experimental yields obtained in Ref. [1] for $^{90-92}$Kr and ^{139}Xe; empty squares: the theoretical values of $^{87-95}$Kr and $^{133-146}$Xe normalised to the ^{91}Kr experimental value; empty circles: theoretical values belonging to $^{90-92}$Br and $^{139-142}$I; stars: hypothetic values for ^{147,148}Xe. E^*= 10 MeV

A serie of parameters can be taken into consideration in order to fit with experimental data [15]: on one hand, the macroscopic kinetic energy $E_{\rm mac}$ which is distributed among the generalized coordinates of the system and it is lost surpassing the barrier, and on the other hand some parameters of the model as the surface diffusivity entering in the calculation of the macroscopic potential barrier computed with the Yukawa–plus–exponential formula or the value of the l^2-coupling coefficient belonging to the two–center microscopic model [16]. We choosed to try a fit by variations of the last two parameters entering in the potential end keeping the macroscopic kinetic energy non-perturbed (fixed at 1.5 MeV). This choice is justified by Ref. [16] where it is affirmed that for nuclei advancing towards the neutron drip line the l^2–coupling coefficient dumps and the microscopic potential becomes similar to a simple oscillator. In the same time, the diffusivity of the surface term increases. Comparisons with yields available for ^{238}U fission [15] for even–even fragments show that if the coefficient a_s is increased with 0.0005 MeV with the addition of one neutron when the nucleus has more than 4 neutrons in excess relatively to the stable isotope, the theoretical

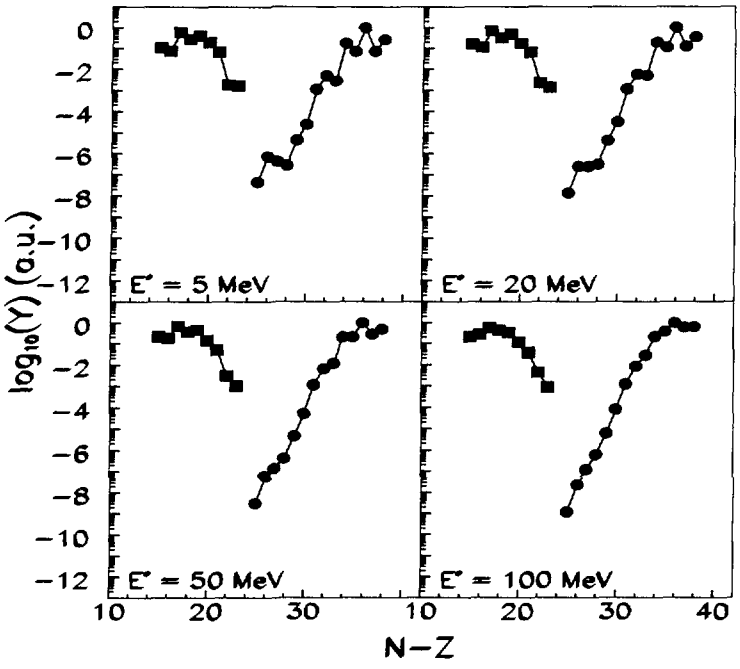

Figure 5: The logarithmic yields in arbitrary units of Kr (squares) and Xe (circles) versus the difference between neutrons and protons at different excitation energies E^* for the fission of ^{239}U. For the normalisation, the logarithm of the maximum yield is 0 in each plot.

results are in good agreement with the experiment. The tests realised by vanishing the l^2–coupling term destroyed the agreement previously obtained with the experimental data by varying only a_s.

This version of the STCM constructed for large mass–asymmetries is unable to compute the splitting in two fragment with approximatively equal masses without appreciable errors. In this work, it is the reason for a lack of information for nuclei with masses near 120.

Anyhow, information about the dependence of the variations of the yields for different nuclides in different areas of the nuclear chart versus the excitation energy of the parent nucleus are provided. In this work, the attention is focussed on the Z=36 (Kr) and Z=54 (Xe) isotopes since an experiment has been performed in the frame of our project [1] in order to estimate the noble gases neutron rich nuclei production. Results obtained for prompt fission Kr and Xe products are presented in figure 4 for a wide range of masses and for E^*=10 MeV. The theoretic yields are normalized to the experimental value obtained for ^{91}Kr. The experimental data from Ref. [1] are plotted with filled symbols. Also, the theoretical value determined for ^{139}I prompt fission relative yield is plotted and it is very close to the experimental ^{139}Xe value. It is known [17] that ^{139}I ($T_{1/2}$=2.3 s) decays by β–emission in ^{139}Xe and contributes to the yield of this isotope and, in figure 4, matches the experimental value, if the yields are considered to be provided only by binary prompt fission products. Because precise data for the γ–rays of ^{139}I are not available, we may study its production in a future experiment of our project once a on–line mass–separator becomes available. Also theoretical expectations for $^{90-92}$Br and $^{139-140}$I are plotted. The $^{90-92}$Br yields are too low to infer the values measured for Kr while the $^{139-142}$I yields compete with the final productions of ^{139,140}Xe. In figure 4, two stars indicate theoretical results for ^{147,148}Xe isotopes which are unstable prompt fragments and therefore are not good candidates for radioactive beams. In consequence, these two isotopes are not very

interesting in the context of our experiment but their representation indicates that Xe theoretic yields begin to decrease near the neutron drip line. If we consider that 2 or 3 neutrons are emitted in each fission event, once again, the theoretical values agree with the experimental ones as it will be discussed below.

In figure 5, the relative Kr and Xe yields (Y) obtained from our code are displayed in a logarithmic scale for a set of excitation energies versus the isospin $N - Z$.

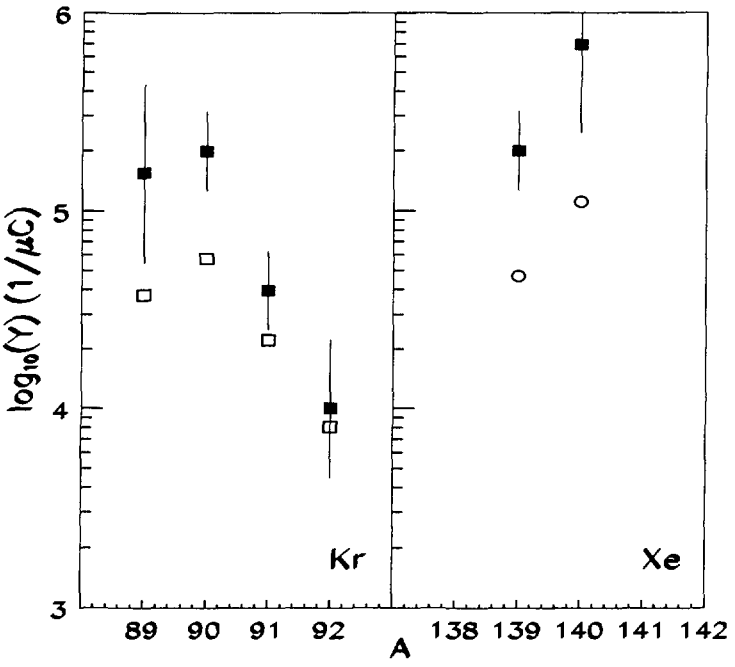

Figure 6: Comparison between experimental and theoretical values obtained after the evaporation of one nucleon.

Let us note, as displayed in figure 5, that the slope of the decrease of the Kr neutron rich isotope production becomes more accentuated as the excitation energy is increased. Thus, for the production of Kr neutron rich isotopes lower excitation energies must be preferred. The production of neutron rich Xe isotopes is always close to the maximum value obtained for Kr.

In the case of fission, it is expected that the intrinsec excitation energies will be shared between the two nascent fragments proportionally to their masses. As an example, for a hypothetic total excitation energy of 100 MeV, about 60 MeV will be taken by the heavy fragment (Xe in our case). This energy will be lost by nucleon evaporation and the prompt products formed will be shifted towards the stability. It could be expected from the trends displayed that the neutron rich heavy fragments will not survive the evaporation process whereas for excitation energies below 20 MeV, the neutron rich heavy fragments are more likely to be observed. At low excitation energies, in average 2.5 nucleons are emitted per fission event in a channel with masses 90 and 140 for the light and the heavy fragment, respectively. It can be deduced that these nucleons are almost equally distributed between fragments [18, 19]. In figure 6, the experimental Kr and Xe (unpublished values belonging to ^{140}Xe and ^{89}Kr are added) values are compared with the theoretical yields for Kr and I extracted from figure 4. Here, the theoretical yields are shifted with the release of one neutron to simulate the evaporation (for example, the theoretical yield belonging to ^{91}Kr is now plotted in the location of ^{90}Kr). The similitude between experimental and

theoretical relative trends is remarkable (remember that the model provides only relative values between the yields). In these circumstances, it is tempting to assume that the β–decay of the ^{140}I ($T_{1/2}$=0.86 s) and ^{141}I ($T_{1/2}$=0.43 s) primary fission products widely participate to the observed yields of ^{139}Xe and ^{140}Xe, respectively. This discussion and this simple interpretation of our results favor an excitation energy for the production of neutron rich nuclei which can be choosed below 20 MeV. The same trends can be deduced from Ref. [15] where almost all the fission products for ^{238}U projectile were measured.

Finally, this code provides estimations of the relative probabilities of different binary fission channels for a parent nucleus (A_0, Z_0) split into two spherical fragments (A_1, Z_1) and (A_2, Z_2). At this stage, the prompt neutron emission and evaporation are not accounted for, but latter simulation of one neutron evaporation can provide reasonable understandings of the experimental results. The probability of a binary channel characterized by a given mass asymmetry is proportional to the simple WKB penetrability formula for penetration through the barrier between the turning points. The only required parameters are the mass number, the atomic number and the excitation energy of the parent nucleus, the mass numbers and the atomic numbers of the nascent fragments, the remaining parameters being deduced by a fitting procedure.

References

[1] F. Clapier, A.C. Mueller, J. Obert, O. Bajeat, M. Ducourtieux, A. Ferro, A. Horbowa, L. Kotfila, C. Lau, H. Lefort, S. Kandri–Rody, N. Pauwels, J.C. Potier, J. Proust, J.C. Putaux, C.F. Liang, P. Paris, A.C.C. Villari, R. Lichtenhäler, L. Maunoury and J. Lettry, submited to Z.Phys. A.

[2] Concept for an advanced exotic beam facility based on ATLAS, working paper, Physics Division, Argonne National Laboratory, February 1995.

[3] Report on the European Radioactive Beam Facilities from the NuPECC study group, R.H. Siemssen convenor et al., G.E. Körner ed., NuPECC, München, (1993).

[4] Report on the European Radioactive Beam Facilities from the NuPECC study group, A.C. Mueller convenor et al., (1997).

[5] M.Mirea, D.N.Poenaru and W.Greiner, Z.Phys. A **349**, 39 (1994).

[6] K.T.R. Davies and J.R. Nix, Phys.Rev. C **14**, 1977 (1976).

[7] D.N. Poenaru, M. Ivaşcu and D. Mazilu, Comp.Phys.Comm. **19**, 205 (1980).

[8] P. Möller and J.R. Nix, At. Data. Nucl. Data Tables **26**, 165 (1981).

[9] M. Mirea, Phys. Rev. C **54**, 302 (1996).

[10] M.Mirea and F. Clapier, Europhys.Lett. **40**, in press, (1997).

[11] M. Brack, J. Damgaard, A. Jensen, H. Pauli, V. Strutinsky and W. Wong, Rev. Mod. Phys. **44**, 320 (1972).

[12] I. Ragnarsson, in Proceedings of the International Conference of Properties of Nuclei Far from the Region of Beta Stability, Leysin, CERN Report No. 1970–30, 1970, p. 847.

[13] H.J. Lustig, J.A. Maruhn and W. Greiner, J.Phys.G **6**, L 25 (1980).

[14] D.L. Hill and J.A. Wheeler, Phys. Rev. **89**, 1102 (1953).

[15] C. Donzaud, S. Czajkowski, P. Armbruster, M. Bernas, C. Bockstiegel, Ph. Dessagne, H. Geissel, E. Hanelt, A. Heinz, C. Kozhuharov, C. Miehe, G. Munzenberg, M. Pfutzner, W. Schwab, C. Stephan, K. Summerer, L. Tassan–Got and B. Voss, International Meeting on Properties of Nuclei far off the Stability Valley, Obninsk, Russie, 10-13 june 1997, Report IPNO DRE 97–19.

[16] J. Dobaczewski, I. Hamamoto, W. Nazarewitz and J.A. Sheikh, Phys. Rev. Lett. **72**, 981 (1994).

[17] C.M. Lederer and V. Shirley, Tables of Isotopes, Seventh Ed., John Wiley & Sons, 1978.

[18] M. Lefort, Chimie Nucléaire, Dunod, Paris, 1966.

[19] H.W. Schmitt, R.W. Lide and F. Pleasonton, NIM **63**, 237 (1968).